

Analytical Methods

Accepted Manuscript



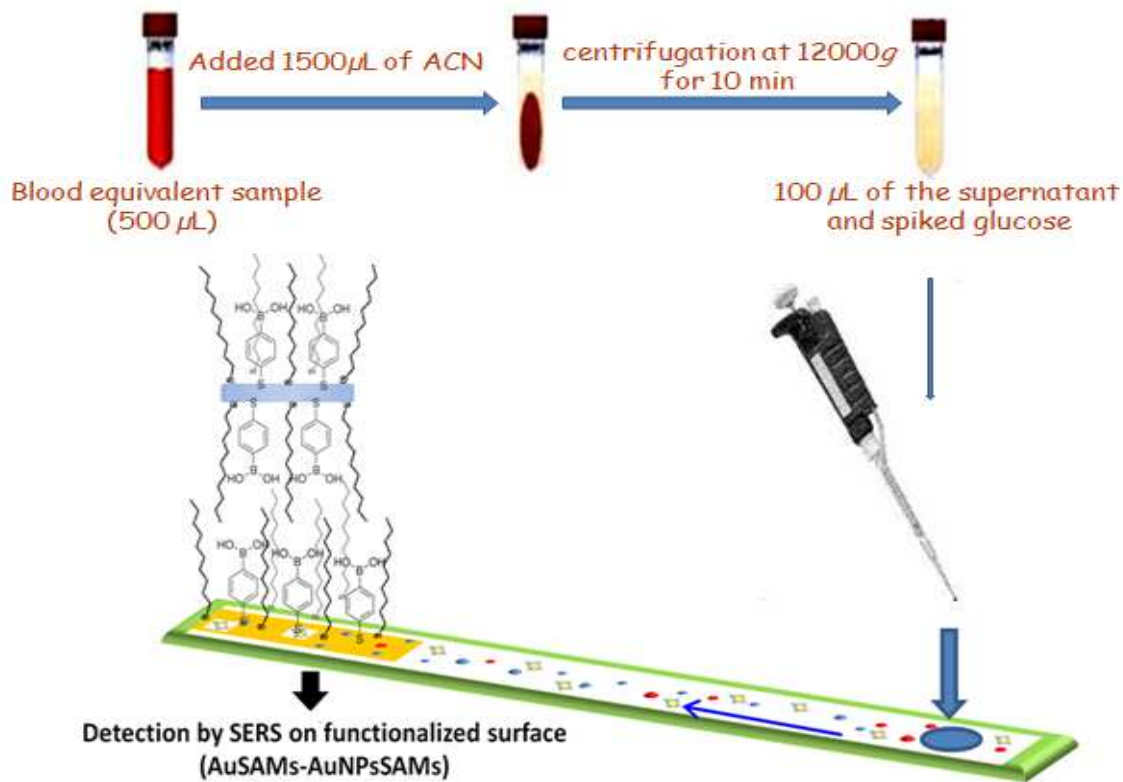
This is an *Accepted Manuscript*, which has been through the Royal Society of Chemistry peer review process and has been accepted for publication.

Accepted Manuscripts are published online shortly after acceptance, before technical editing, formatting and proof reading. Using this free service, authors can make their results available to the community, in citable form, before we publish the edited article. We will replace this *Accepted Manuscript* with the edited and formatted *Advance Article* as soon as it is available.

You can find more information about *Accepted Manuscripts* in the [Information for Authors](#).

Please note that technical editing may introduce minor changes to the text and/or graphics, which may alter content. The journal's standard [Terms & Conditions](#) and the [Ethical guidelines](#) still apply. In no event shall the Royal Society of Chemistry be held responsible for any errors or omissions in this *Accepted Manuscript* or any consequences arising from the use of any information it contains.

Graphical abstract



1
2
3
4
5
6
7
8
9
10
11
12
13
14
15
16
17
18
19
20
21
22
23
24
25
26
27
28
29
30
31
32
33
34
35
36
37
38
39
40
41
42
43
44
45
46
47
48
49
50
51
52
53
54
55
56
57
58
59
60

Glucose determination based on two component self-assembled monolayer functionalized surface-enhanced Raman spectroscopy (SERS) probe

5 Hilal Torul^a, Hakan Çiftçi^b, Fahriye Ceyda Dudak^c, Yekbun Adıgüzel^d, Haluk Kulah^{d,e}, İsmail Hakkı Boyacı^c and Uğur Tamer^{*a}

10 In this report, we present a new detection method for blood glucose, using gold nanorod SERS; Surface enhanced Raman scattering probe embedded in two component Self-assembled monolayers (SAMs). Gold nanorod particles and gold coated slide surface were modified with the two component SAMs consisting of 3-mercaptophenylboronic acid (3-MBA) and 1-decanethiol (1-DT). The immobilization of 3-MBA/1-DT surface-functionalized, gold nanoparticles onto 3-MBA/1-DT modified, gold-coated 15 slide surfaces was achieved by the cooperation of hydrophobic forces. Two component SAM functionalized substrates were used as the SERS probe, by means of the boronic acid and the alkyl spacer functional groups that serve as the molecular recognition and penetration agents, respectively. SERS platform surface was characterized by cyclic voltammetry, contact angle measurements, AFM; atomic force microscopy and Raman spectroscopy. Optimum values of the parameters such as pH, time and (3-MBA/1-DT) molar ratio were also examined for the glucose determination. The analytical performance was evaluated and linear calibration graphs were obtained in the glucose concentration range of 2-16 mM, which is also in the range of the blood glucose levels, and the detection limit was found to be 0.5 mM. As a result, the SERS platform was also used for the determination of glucose in plasma samples.

25 **Keywords:** Gold nanoparticles, Self-assembled monolayer, Boronic acid, Surface enhanced Raman scattering, Partition layer, Glucose

Introduction

30 Determination of glucose in body fluids is an important analytical challenge in diagnostic analysis, especially in the case of continuous monitoring of the glucose level in diabetes mellitus patients.¹ Although enzymatic assays have been generally used for glucose determination, the most serious problem of this approach is the lack of enzyme stability.^{2,3} For this reason, new molecular recognition systems for the 35 detection of glucose molecule have been attracting considerable attention.²⁻⁶ A molecular recognition agent, phenylboronic acid, represents an ideal synthetic molecular receptor, for its ability to recognise the cis-diol configuration in saccharides and to form reversible covalent complexes with 40 saccharides in aqueous media.⁷⁻¹⁰ Phenylboronic acid derivatives have been used for saccharide sensing applications in various methods, utilizing piezoresistive microcantilevers⁷⁻⁹, UV-Vis absorption¹⁰, fluorescence measurements^{11,12}, electrochemistry^{13,14}, plasmonics^{15,16}, holography and SPR¹⁷⁻²². 45 Consequently, phenyl boronic acid probes inherently has the potential to be used as the recognition moiety for the detection of glucose in a complex matrix such as blood.

50 SERS provides high sensitivity and selectivity when dealing with low volume samples and low concentration target analytes²³⁻³³. However, SERS based analytical methods or sensors are still limited to research laboratories. The main reason is the difficult control of nanostructure surface or nanoparticle with Raman activity³⁴. Because the signal

55 enhancement results from an electric field in close proximity to a nanostructure surface and the electric field is localized between nanoparticles or metal film. In addition, the intensities of SERS signals are also based on the aggregation of nanoparticles³⁵. There is still much effort to develop reliable and reproducible SERS based analytical methods. The 60 determination of glucose using SERS was reported in a recent work by Van Duyne group who demonstrated the direct detection of glucose using SERS by partitioning the glucose into alkanethiolate monolayers, such as decanethiol and (1-mercaptopundeca-1(-yl) tri (ethylene)glycol).³⁶⁻³⁹ The alkyl spacer functional group was used to increase the glucose permeation, during direct detection of glucose using SERS.

65 SAMs offer a number of advantages as suitable platforms for surface modifications that serve to attach biological molecules onto nanoparticle surfaces.⁴⁰ They form structurally 70 well-defined and compact monolayers on the surfaces of the nanoparticles. The experimental procedure for the formation of SAMs from dilute ethanolic solution is straightforward and applicable to most sensor configurations. For instance, 3-aminophenylboronic acid (APBA) was immobilised on a gold 75 electrode via a SAM and the change in capacitance of the sensing surface caused by the binding between 3-APBA and bacteria was detected in a flow-through system, by a potentiostatic step method.²² This method is not specific to the bacteria type, it shows binding of bacteria to the 3-APBA. 80 The complexation of saccharides with aromatic boronic acids produces a stable ester and the binding constant is dependent

on the pH, electrolyte concentration and pKa of the aromatic boronic acid.⁴¹ Application of this method utilizing 3-APBA was also offered as means for a rapid detection of total bacteria since the cell wall of bacteria consist of polysaccharides with diol-groups that can chemoselectively bind to 3-APBA.^{42,43} In our previous study, surface functionalized gold nanoparticles with MUA and 4-mercaptophenyl boronic acid (MBA) were immobilized onto poly(3-octylthiophene) (POT) by hydrophobic forces and the POT-Au-SEM electrode that have been prepared was used for glucose determination as a potentiometric non-enzymatic glucose sensor, which was based on the partitioning of glucose into the boronic acid/decanethiol layer.⁴⁴ In a similar manner, a new conducting polymer organic electrode, poly(3-aminophenylboronic acid-co-3-octylthiophene), was used for the determination of glucose as well, and the analytical performance of the sensor was evaluated with potentiometric measurements.⁹ We also developed a sensor surface based on MBA terminated Ag@Au-graphene oxide nanomaterial, which was used for the determination of glucose, through the complex formation between the boronic acid and diol groups of the glucose.⁴⁵

In this work, we proposed different strategy to construct a SERS template for the sensitive and selective detection of glucose using mixed SAMs modified gold nanoparticles immobilized on mixed SAMs modified gold surfaces. The mixed monolayer of 3-mercaptophenylboronic acid (3-MBA) and decanethiol (1-DT) groups was formed on a gold-coated slide surface and gold nanoparticles surfaces. The immobilization of surface-functionalized SAM gold nanoparticles onto modified, gold-coated slide surfaces was achieved by the cooperation of hydrophobic force. The gold coated slide surface and gold nanoparticle surface was covered with the two components mixed layer of SAM. After mixing, gold nanoparticles can be immobilized to the gold coated slide surface directly due to hydrophobic surface. The resulting SERS platform was used for the determination of glucose through the complex formation between the mixed monolayer and glucose. The SERS platform was characterized by cyclic voltammetry, contact angle measurements, AFM and Raman spectroscopy. The SERS platform was also used for the determination of glucose in plasma samples.

Experimental

Materials

Hydrogen tetrachloroaurate (HAuCl₄), hexadecyltrimethylammonium bromide (CTAB), L-ascorbic acid (AA), 1-decanethiol (DT), 4-mercaptophenyl boronic acid (4-MBA), ascorbic acid (AA), uric acid (UA) and ethanol were purchased from Sigma-Aldrich (Taufkirchen, Germany) and were used as received. Silver nitrate (AgNO₃) and sodium borohydride (NaBH₄) were purchased from Merck (Darmstadt, Germany). All solutions were prepared with deionized water, 18.2 MΩ.cm, which was obtained free from organic matter, from a Millipore purification system. Blood reference material (Hb/glucose L-1) was purchased from Seronorm (Billingstad,

NORWAY). Gold coated silicon wafer was purchased from Sigma-Aldrich (Taufkirchen, Germany). The thickness of the gold layer is 100 nm.

Gold coated slide surface modification

The SAMs of 3-MBA and 1-DT were prepared by immersing the gold-coated slide surface into a 3-MBA and 1-DT mixture solution for 24 h. The concentration of 3-MBA and 1-DT in ethanol was 10 mM, each. After the immobilization process, modified gold-coated slide surface (AuSAMs) was rinsed three times with ethanol, to remove excess 1-DT or 3-MBA.

Synthesis of gold nanorods and surface modification

Gold nanorods were prepared by the previously reported seed-mediated growth technique, with slight modifications.⁴⁶ To prepare rod shaped gold nanoparticles, 4.75 mL of 0.1 M CTAB, 250 μL of 0.01 M HAuCl₄, and 60 μL of 4x10⁻³ M AgNO₃ were mixed, respectively. After that, 250 μL of 0.1 M ascorbic acid was added dropwise to the resulting solution. Then, 5 μL seed solution was added to the stock solution, and this final mixture was stirred for 10 seconds, and allowed to stay for 3 hours at room temperature. The seed solution was prepared by mixing 7.5 mL of 0.1 M CTAB solution with 250 μL of 0.01 M HAuCl₄ solution. Once mixed 600 μL of 0.01 M ice-cold NaBH₄ was added to the resulting solution and allowed to stand for 5 min, to form the seed solution.

Gold nanorods solution was centrifuged to remove excess CTAB from the surface of gold nanorods. After sonication for one hour, the precipitate was centrifuged and washed with deionized water, and the procedure was repeated four times. Based on the TEM images (Supplemental material, Figure S1), the rod shaped gold nanoparticles have an average diameter of 22 ± 3 nm and average length of about 53 ± 4 nm. The resulting particles were dispersed overnight, with a 2 mL ethanol solution containing 10 mM 1-DT and 10 mM 3-MBA, under constant stirring, and cleaned three times with ethanol solution, to remove the excess 1-DT and 3-MBA.

Preparation of SERS platform

Au SAMs surfaces dipped into gold nanoparticle (AuNPs) SAMs containing 2 mL ethanol solution, for 5 min, for immobilization of AuNPs SAMs on to Au SAMs surface, by the aid of hydrophobic forces. The resulting platform (Au SAMs-AuNPs SAMs) (Scheme 1) was cleaned three times with ethanol, to remove the excess nanoparticles. Au SAMs-AuNPs SAMs surface was characterized by cyclic voltammetry. A Gamry potentiostat (model reference 600,) was used to perform cyclic voltammetry measurements. Au, Au SAMs and Au SAMs-AuNPs SAMs surfaces were visualized with AFM (XE-100E; Park Systems Corp., Suwon, Korea). The measurements were performed in the non-contact mode, by using 910 M-NSC14/Cr Au-type cantilevers, with 0.3 to 0.5-Hz scanning speed. Prior to the AFM measurements, the surfaces were washed with ultrapure water and allowed to dry in air.

The static contact angles of water drops on the Au SAMs and Au SAMs–AuNPs SAMs surfaces were measured at room temperature, with an automatic contact angle analyzer, combined with flash camera equipment (model DSA 100, Krüss, Germany). All the contact angles presented here were an average of five measurements.

10 Surface Plasmon Resonance measurements

Binding of glucose to Au SAMs and Au SAMs–AuNPs SAMs surfaces was investigated by Spreeta™ SPR sensor (Texas Instruments, Dallas, TX, USA), combined with three-channel flow cell and 12-bit DSP control box. The flow of the reagents was controlled by syringe pumps (Goldman Pump, Biasis Ltd. Sti., Ankara, Turkey) and four-way switching valves (Upchurch Scientific, Oak Harbor, WA, USA). Self-assembled monolayer (SAM) was formed on the gold coated sensor surfaces by incubating the sensor overnight, with 10 mM 1–DT and 10 mM 3–MBA, in absolute ethanol. After establishing the baseline with borate buffer (pH 9.0), four different concentrations of glucose, ranging from 2.8 μM to 22.2 μM , were injected to the sensor surface, at a flow rate of 25 $\mu\text{L min}^{-1}$. The binding curves were generated by taking the difference of the binding measurement and the control measurement, in which the glucose solutions were injected to blocked surface. The curves were fitted to a simple Langmuir binding model, in order to determine the binding constant between the boronic acid and glucose.

Glucose measurements using SERS platform

DeltaNu Examiner Raman microscope (Deltanu Inc., Laramie, WY, USA) with a 785–nm laser source, a motorized microscope stage sample holder, and a CCD detector was used to determine the glucose concentration. Varying concentrations of 10 μL glucose solutions were dropped on the Au SAMs–AuNPs SAMs surface and after letting it dry on the surface for 5 min, this surface was rinsed three times with water to remove the unbound glucose molecules. Then, SERS spectrum was acquired in the 500–1800 cm^{-1} range. During the measurements, a 20 X objective was used and the laser spot diameter was approximately 30 μm . Samples were measured with 140 mW laser power, for 30 s acquisition time. Baseline correction was performed for all measurements. Spectral intensity was obtained from five different locations of the substrate and was averaged. The change in intensity values of the fundamental peaks of Au SAMs–AuNPs SAMs surface was monitored both before and after the addition of glucose.

The addition of organic solvents to serum results in the precipitation of high molecular weight proteins, leaving the low molecular weight molecules behind, in solution. In this study, acetonitrile (ACN) was used for the precipitation of major serum protein components. Blood reference material (500 μL) was transferred to a centrifuge tube and 1500 μL of ACN was added into the tube. The protein precipitate was pelleted by centrifugation at 12000g, for 10 min, at room

temperature. The supernatant was transferred to a clean tube. Five different concentrations of glucose, ranging from 0 to 8mM, were prepared with 0.1 M borate buffer (pH 9.0) and 100 μL of the supernatant was added to each tube. The final volume of the samples was completed to 1000 μL with 0.1 M borate buffer (pH 9.0). The prepared sample solutions were vortexed to mix the constituents. They were then dropped on Au SAMs–AuNPs SAMs surface and after letting it dry on the surface for 5 min, the surfaces washed three times with water to remove the unbound glucose molecules. Then, SERS spectrum was acquired in the range of 500–1800 cm^{-1} .

Results and Discussion

Design strategy for glucose sensor

The schematic of the surface composition of the SERS platform for the determination of glucose is shown in Scheme 1. The gold chip surface was modified with mixed monolayer of 3–MBA and 1–DT and the gold nanorod particles that were modified with mixed SAM were embedded to the surface by hydrophobic force. Alkyl groups and boronic acid are needed for the penetration of glucose molecules into the sensing surface since an alkanethiolate group can act as a partition layer and phenylboronic acid groups as a complex forming agent on the resulting substrates.⁹ Accordingly, the use of multi–component SAM of 3–MBA and 1–DT on gold chip surface provided the direct and enhanced immobilization efficiencies of gold nanorod particles.

In the present work, we have used $\text{Fe}(\text{CN})_6^{4-}$ as a redox probe, to evaluate the entirety of resulting SERS platform and cyclic voltammetry was employed to study the electron transfer process on the SAMs modified electrodes and gold coated slide, which covered with the SAMs (Scheme 1), cannot touch the solution directly due to hydrophobic surface. Figure 1 shows the voltammogram of ferrocyanide redox reaction taken from the mixed monolayer of 3–MBA and 1–DT surface. It was observed that multi–component SAMs completely block ferrocyanide redox reaction showing the full coverage of SAMs on gold surface (Figure 1, voltammogram c). Figure 1a shows the typical behavior of ferrocyanide on bare gold electrode. On the other hand, after interaction of gold nanorod particles, a CV of ferrocyanide redox reaction was observed as shown in Figure 1 (voltammogram b) indicating that ferrocyanide molecules could penetrate into the monolayer and the electron could transfer through the SAMs via tunneling process due to presence of gold nanoparticles embedded in SAMs.

Contact angle measurements were used for the characterization of SERS platform surfaces in terms of hydrophobicity. Fundamentally, the more hydrophobic the surface is, the smaller is the contact area of a water droplet on it and therefore, the larger is the value of the contact angle. The boronic acid end–groups of modified surfaces lead to characteristic changes in the polarity of the surfaces. Therefore, we performed contact angle measurements to quantify the corresponding changes after modification with gold nanorod particles as well. As expected, gold surface is hydrophilic and

1 water contact angle of the bare gold surface is 8.51°
2 (Supplemental material, Figure S2a). Contact angles of
3 AuSAMS (Supplemental material, Figure S2b) and Au SAMS–
4 AuNPs SAMs (Supplemental material, Figure S2c) surfaces
5 were found to be 74.9° and 58.3° , respectively. The change in
6 the contact angle values according to the SAM type on the gold
7 surface indicated that the surface modification has occurred
8 and the surface hydrophobicity increases with the addition of
9 the decanethiol. When the mixed monolayer modified gold
10 nanorod particles were added on the AuSAMS surface, the
11 numbers of boronic acid end-groups were increased and the
12 resulting contact angle value was decreased.

13 We carried out the experiments regarding the stability of
14 the prepared sensor. We did not observe any SERS signal
15 intensity change within the two months using the prepared
16 SERS probe. The intensity change of SERS peak was
17 demonstrated in the Figure S3.

18 The detailed characterization of gold nanorod particles
19 used in this study was reported in our previous study.⁴⁴ The
20 functional group on the nanoparticle is an important factor
21 affecting the immobilization efficiencies of gold nanorods onto
22 the gold chip surface. AFM measurements were also
23 performed to demonstrate the existence and appropriate
24 immobilization of AuNPs SAMs on Au SAMS surface. It can
25 be seen in Figure 2a that the roughness increased slightly after
26 the self-assembly of 3-MBA and 1-DT monolayers on the
27 surface (Figure 2b). The addition of AuNPs SAMs to Au
28 SAMS surface result in considerable increase in roughness and
29 the size of the knobs is consistent with the size of the AuNPs
30 SAMs size (Figure 2c). AFM images show that nanoparticles
31 on the AuSAMS surface had a homogenous distribution.

32 Interaction between glucose and SERS platform

33
34
35 To explain the glucose penetration to the platform surface
36 SERS measurements were carried out. Significant SERS peaks
37 were observed at 698, 1000, 1024, 1070, 1184, 1290, 1490,
38 1583 cm^{-1} on Au SAMS–AuNPs SAMs surfaces as shown in
39 Figure 3. The Raman band appeared at 698 cm^{-1} and small
40 peaks at 1024 cm^{-1} were due to C–S stretching mode and the
41 peak at 1000 cm^{-1} was due to phenyl groups.^{47,48} The peaks at
42 1290 and 1490 cm^{-1} were attributed to C–C and C=C
43 stretching modes of the phenyl groups, respectively.⁴⁹ Raman
44 bands at 1070 cm^{-1} and 1184 cm^{-1} illustrated the B–OH and
45 B–C stretching modes, respectively.⁵⁰

46 The interaction of boric and boronic acid derivatives with
47 saccharides is well documented.⁵¹ Boronic functional groups
48 participate in complexing with compounds containing vicinal
49 diols, through reversible ester formation. In our previous
50 study, we demonstrated that the alkyl groups are needed to
51 penetrate the glucose molecule onto SAM film surface.⁴⁴ The
52 main advantage of the decanethiol is to provide as a partition
53 layer near the film surface for the effective preconcentration of
54 glucose. A control experiment using only boronic acid
55 functional group displayed less signal change in SERS
56 response (data not shown). For this reason, the two component
57 mixed monolayer of SAM functionalized substrate was used as
58 the SERS probe. With the addition of increasing glucose

concentration on the Au SAMS–AuNPs SAMs surface, B–OH
60 peak intensity at 1070 cm^{-1} was decreased as shown in Figure
3. The decrease of Raman band intensity revealed that glucose
was partitioned into the platform surface and formed a
complex with the phenylboronic acid group. The result also
showed that the Au SAMS–AuNPs SAM surface can be used
65 as a glucose sensor by SERS measurement.

Immobilization of AuNPs SAMs on Au SAMS surface
provides high SERS signals upon binding of glucose to sensing
surface. In order to reveal this signal enhancement, binding
affinities of glucose to Au SAMS and Au SAMS–AuNPs SAMs
70 surfaces were determined using SPR sensor. The binding
affinity of glucose to the sensing layer obtained from SPR
measurements confirm the result that glucose bind to Au
SAMS–AuNPs SAMs surface with a higher affinity than
binding to the Au SAMS surface. Different concentrations of
75 glucose solutions (pH 9.0, 100 mM borate buffer) were
injected both to the Au SAMS surface (Figure 4a) and Au
SAMS–Au NPs SAMs surface (Figure 4b), and the binding
data were consistent with simple 1:1 Langmuir interaction
80 model. The affinity constant of glucose-boronic acid complex
on Au SAMS–AuNPs SAMs surface was calculated as 7.7×10^4
 M^{-1} , which is three fold higher than the constant that was
obtained for the Au SAMS surface ($2.5 \times 10^4 \text{ M}^{-1}$). This
enhanced affinity can be the result of immobilization of AuNPs
on the SPR chip surface, as AuNPs are known to increase the
85 sensitivity of SPR systems⁵² and increase the surface area of
interaction, which may lead to a better orientation of the
surface constituents for binding. There was no binding when
the glucose solutions were injected to the gold surface
modified with only 1-DT showing the selective binding of
90 glucose to boronic acid group (data not shown). The binding
constant of glucose-boronic acid complex on 3-MBA modified
gold surface ($3.1 \times 10^4 \text{ M}^{-1}$) was close to the one obtained from
glucose on the Au SAMS surface (data not shown). This result
indicates that partition of glucose was not observed in SPR
95 system, probably because of the continuous flow in SPR.

The complexing produces a stable boronate anion, and a
proton within a pH range of 6–10. The binding constant for
boronic acid-sugar complex increases at higher pH values.⁸
The effect of pH on binding of 4 mM glucose to Au SAM–
100 AuNPs SAM surface was examined within the pH range of
7.0–10.0, in 100 mM borate buffer and maximum glucose
response was obtained at pH 9 (Supplemental material, Figure
S4a). The effect of surface-incubation duration of the glucose
solution on the peak intensity (ΔI) at 1070 cm^{-1} was examined,
105 within the time range of 2–20 min (Supplemental material,
Figure S4b). In case of incubation durations longer than 10
min, the peak intensity was almost constant. Optimum duration
of the incubation was found to be 5 min and used throughout
the study. An analysis time of 5 min is long when compared
110 with non-enzymatic electrochemical glucose sensing methods.
However, this incubation time is critical for the developed
system due to the partition of glucose which provides higher
sensitivity and selectivity.

The effect of the mixed SAMs (1-DT /3-MBA) molar
115 ratio that was incubated on the gold nanorod surface, on the
decrease of the peak intensity (ΔI) at 1070 cm^{-1} was examined

(Supplemental material, Figure S5b). The highest peak intensity, hence the best response was obtained in case of 1-DT /3-MBA (1/3) molar ratio. When the MBA concentration was increased, glucose interaction with the boronic acid groups was increased. Optimum molar ratio was found to be 1-DT /3-MBA (1/3). The effect of the 1-DT /3-MBA molar ratio that was incubated on the gold coated slide surface, on the decrease of peak intensity (ΔI) at 1070 cm^{-1} was also examined (Supplemental material, Figure S5a). As shown in Figure S5, the best response was obtained in case of 1-DT /3-MBA (1/1) molar ratio. With the decrease of 1-DT concentration was decreased amount of modified AuNPs interacting with Au SAMs surface by hydrophobic force and observed glucose response was decreased.

The peak intensity of B-OH at 1070 cm^{-1} was decreased as a function of increasing glucose concentration in the buffer solution that was incubated on the surface, as shown in Figure 3b. Calibration curves were constructed using the standard addition method and the calibration curve was plotted with the changes of the peak intensities (ΔI) of B-OH versus varying glucose concentrations (2–16 mM) (Figure 5). The SERS response between 2 mM and 16 mM was linear, and the detection limit was found to be 0.5 mM, for glucose. The comparison was made between the current systems and developed SERS technique as shown in Table 1. Although the observed LOD value of SERS based technique was found to be high compared to the other sensing systems in the literature, the linear range of SERS based technique presents wider linear detection range. The reproducibility of the method was verified by successive tests for the determination of 4 mM glucose, and the relative standard deviation (RSD) was found as 4.42 % ($n=4$).

It is well-known that glucose coexists with other species in blood sample and it is important to develop a SERS method for selective determination of glucose in the presence of other interferences. Here, SERS response of proposed platform was examined in the presence of possible interference, namely ascorbic acid (AA), uric acid (UA), and dopamine (DA). The physiological level of glucose is about 50 times higher than that of interfering species. Therefore, 4 mM glucose was added to the solutions, along with different concentrations of interfering agents ranging between 0.1 mM and 0.4 mM, and glucose response was determined through the peak intensity of B-OH at 1070 cm^{-1} . Interfering agents in this range had a small effect on the peak intensity at 1070 cm^{-1} (Supplemental material, Figure S6). The changes in intensity of SERS signal of B-OH were found to be 14%, 22% and 13% for UA, DA and AA respectively. These results showed that the proposed SERS based detection method can be used for selective detection of glucose in the presence of up to 0.4 mM UA, AA and DA.

Application in serum sample

In order to establish the accuracy of the proposed procedure, the method has been applied to the determination of glucose in the certified blood reference material. After appropriate dilution, we tested the concentration of glucose of blood reference material, using the standard additions method, as

shown in Figure 5. The calibration graph was used for direct determination of blood glucose. The concentration of glucose in the reference material was found as 5.20 ± 0.40 and the certified value for glucose was 6.17 ± 0.11 . Within a 95% confidence interval, the glucose concentration value calculated experimentally from the calibration graph and the certified glucose concentration value of the sample in the product data sheet are not statistically different. The compatibility between the two results proves the reliability of this sensor for determination of the glucose concentration in real samples. So, the proposed method provided a new potential platform for developing a SERS-based, non-enzymatic sensor for glucose determination.

Conclusion

SERS is a highly sensitive and selective method that can be utilized for rapid and quantitative detection of glucose. A simple, SERS-based approach for the determination of glucose concentration is presented in this paper. This work reports our improvements in the SERS measurements of glucose, based on a 1-decanethiol group that acts as a partition layer on hydrophobic substrates and the phenyl boronic acid group, serving as a complexing agent for preconcentrating glucose. We have successfully demonstrated the feasibility of a SERS sensor for sensitive glucose detection, by the use of non-enzymatic reactions. Results concluded that the SERS sensor can be used for glucose determination in the presence of interferences as well. Serum sample analysis was also performed for glucose detection in the certified blood reference material and the results were in good agreement with the reported value in the reference material. Based on these results, it is demonstrated that the developed sensor can be used for the detection of glucose in blood.

Acknowledgements

Authors acknowledge The Scientific and Technological Research Council of Turkey (TUBITAK) with the project number Cost MP 1205-111T983 for funding. The authors would like to thank Prof. Nihal Aydođan and Hande Ünsal (Hacettepe University, Department of Chemical Engineering, Turkey) for AFM measurements.

Notes

^aGazi University, Faculty of Pharmacy, Department of Analytical Chemistry 06330, Ankara, TURKEY

^bKırıkkale University, Kırıkkale Vocational High School, Department of Chemistry and Chemical Processing Technologies, 71450 Yahşihan, Kırıkkale, TURKEY

^cDepartment of Food Engineering, Hacettepe University, Beytepe, 06512, Ankara, TURKEY

^dMETU-MEMS Research and Application Center, Middle East Technical University (METU), Ankara, TURKEY

^eDepartment of Electrical and Electronics Engineering, Middle East Technical University, Üniversiteler Mah., Dumlupınar Bulv. No: 1, 06800 Cankaya, Ankara, TURKEY

*Correspondence: Uğur Tamer, E-Mail: utamer@gazi.edu.tr

Gazi University, Faculty of Pharmacy, Department of Analytical Chemistry 06330, Ankara, TURKEY,
 Fax: 903122235018
 Tel: 903122023105

References

- 1 G. Reach, G.S. Wilson, *Anal. Chem.*, 1992, **64**(6), 381A-386A.
- 10 2 M.M.G. Antonisse, D.N. Reinhoudt, *Chem. Commun.*, 1998, 443-448.
- 3 S. Park, H. Boo, T.D. Chung, *Anal. Chim. Acta.*, 2006, **556**, 46-57.
- 4 P.D. Beer, P.A. Gale, *Angew. Chem. Int. Ed.* 2001, **40**(3), 486-516.
- 15 5 B. Linton, A.D. Hamilton, *Chem. Rev.*, 1997, **97**(5), 1669-1680.
- 6 R.R. Klinke, B. König, *J. Chem. Soc., Dalton Trans.*, 2002, 121-130.
- 20 7 G.A. Baker, R. Desikan, T. Thundat, *Anal. Chem.*, 2008, **80**, 4860-4865.
- 8 Ö. Torun, F. C. Dudak, D. Baş, U. Tamer, İ.H. Boyacı, *Sensors and Actuators B*. 2009, **140**, 597-602.
- 9 H. Çiftçi, U. Tamer, M. Şen Teker, N. Özçiçek Pekmez, *Electrochimica Acta.*, 2013, **90**, 358-365.
- 25 10 R. Badugu, J.R. Lakowicz, C.D. Geddes, *Dyes Pigm.*, 2006, **68**, 159-163.
- 11 S. Çubuk, E. Kök Yetimoğlu, M. Vezir Kahraman, P. Demirbilek, M. Fırlak, *Sensors and Actuators B: Chemical.*, 2013, **181**, 187-193.
- 30 12 K.M.K. Swamy, Y.J. Jang, M.S. Park, H.S. Koh, S.K. Lee, Y.J. Yoon, J. Yoon, *Tetrahedron Letters.*, 2005, **46**, 3453-3456.
- 13 S. Aytac, F. Kuralay, İ.H. Boyacı, C. Unaleroğlu, *Sensors And Actuators B.*, 2011, **160**, 405-411.
- 35 14 J. Li, Y.Q. Sun, Y.M. Wei, J.B. Zheng, *Chinese Chemical Letters.*, 2013, **24**(4), 291-294.
- 15 H.B. Liu, Q.Yan, C. Wang, X. Liu, C. Wang, X.H. Zhou, S.J. Xiao, *Colloids and Surfaces A: Physicochemical and Engineering Aspects.*, 2011, **386**, 131-134.
- 40 16 M. Lee, T.I. Kim, K.H. Kim, J.H. Kim, M.S. Choid, H.J. Choie, K. Koh, *Anal. Biochem.* 2002, **310**, 163-170.
- 17 M. Lee, T.I. Kim, K.H. Kim, J.H. Kim, M.S. Choid, H.J. Choie, K. Koh, *Anal. Biochem.*, 2002, **310**, 163-170.
- 45 18 N. Soh, M. Sonezaki, T. Imato, *Electroanalysis.*, 2003, **15**, 1281-1290.
- 19 M.C. Lee, S. Kabilan, A. Hussain, X.P. Yang, J. Blyth, C.R. Lowe, *Anal. Chem.*, 2004, **76**, 5748-5755.
- 20 G.J. Worsley, G.A. Tourniaire, K.E.S. Medlock, F.K. Sartain, H.E. Harmer, M. Thatcher, A.M. Horgan, J. Pritchard, *Clin. Chem.*, 2007, **53**, 1820-1826.
- 50 21 X.P. Yang, M.C. Lee, F. Sartain, X.H. Pan, C.R. Lowe, *Chem. Eur. J.*, 2006, **12**(33), 8491-8497.
- 22 J.M. De Guzman, S.A. Soper, R.L. McCarley, *Anal. Chem.*, 2010, **82** (21), 8970-8977.
- 55 23 S. Nie, S.R. Emory, *Science.*, 1997, **275**, 1102-1106.
- 24 C.R. Yonzon, C.L. Haynes, X. Zhang, J.T. Walsh Jr., R.P. Van Duyne, *Anal. Chem.*, 2004, **76**(1), 78-85.
- 25 X. Zhang, M.A. Young, O. Lyandres, R.P. Van Duyne, *J. Am. Chem. Soc.*, 2005, **127**, 4484-4489.
- 60 26 O. Lyandres, N.C. Shah, C.R. Yonzon, J.T. Walsh Jr., M.R. Glucksberg, R.P. Van Duyne, *Anal. Chem.*, 2005, **77**, 6134-6139.
- 27 D.A. Stuart, C.R. Yonzon, X. Zhang, O. Lyandres, N. Shah, M.R. Glucksberg, J.Y. Walsh, R.P. Van Duyne, *Anal. Chem.*, 2005, **77**, 4013-4019.
- 65 28 G.C. Schatz, R.P. Van Duyne, *New York, USA: John Wiley and Sons*, 2002, vol. 1, 759-774.
- 29 C. Siemes, A. Bruckbauer, A. Goussev, A. Otto, M. Sinther, A. Pucci, *J. Raman Spectrosc.*, 2001, **32**(4), 231-239.
- 70 30 M. Graff, J. Bukowska, K. Zawada, *J. Electroanal. Chem.* 2004, **567**, 297-303.
- 31 U. Kreibig, M. Vollmer, *Springer-Verlag: Heidelberg*, 1995, **25**, 532.
- 75 32 L. Guerrini and D. Graham, *Chem. Soc. Rev.*, 2012, **41**, 7085-7107.
- 33 L. Rodriguez-Lorenzo, L. Fabris, R.A. Alvarez-Puebla, Review Article, 2012, **745**, 10-23.
- 80 34 K.C. Bantz, A.F. Meyer, N. J. Wittenberg, H. Im, Ö. Kurtuluş, S.H. Lee, N.C. Lindquist, S.H. Oh and C.L. Haynes, *Phys. Chem. Chem. Phys.*, 2011, **13**, 11551-11567.
- 35 L. Guerrini, S. Sanchez-Cortes, V.L. Cruz, S. Martinez, S. Ristori and A. Feis, *Journal of Raman Spectroscopy*, 2011, **42**(5), 980-985.
- 85 36 R.G. Nuzzo, F.A. Fusco, D.L. Allara, *J. Am. Chem. Soc.* 1987, **109** (8), 2358-2368.
- 37 M.D. Proter, T.B. Bright, D.L. Allara, C.E.D. Chidsey, *J. Am. Chem. Soc.* 1987, **109** (12), 3559-3568.
- 90 38 J.M. Yuen, N.C. Shah, J.T. Walsh, M.R. Glucksberg, R.P. Van Duyne, *Anal. Chem.*, 2010, **82** (20), 8382-8385.
- 39 K. Ma, J.M. Yuen, N.C. Shah, J.T. Walsh, M.R. Glucksberg, R.P. Van Duyne, *Anal. Chem.*, 2011, **83** (23), 9146-9152.
- 95 40 U. Tamer, D. Cetin, Z. Suludere, İ.H. Boyacı, H.T. Temiz, H. Yegenoglu, P. Daniel, İ. Dinçer, and Yağın Elerman, *Int. J. Mol. Sci.* 2013, **14**(3), 6223-6240.
- 41 K.E. Shafer-Peltier, C.L. Haynes, M.R. Glucksberg, R.P. Van Duyne, *J. Am. Chem. Soc.*, 2003, **125**, 588-593.
- 100 42 C.R. Yonzon, C.L. Haynes, X. Zhang, J.T. Walsh, R.P. Van Duyne, *Anal. Chem.* 2004, **76**, 78-85.
- 43 R.G. Nuzzo, D.L. Allara, *J. Am. Chem. Soc.*, 1983, **105**, 4481-4483.
- 105 44 H.Çiftçi, U.Tamer, *React. Func. Polym.* 2012, **72**, 127-132.
- 45 V.K. Gupta, N. Atar, M. L. Yola, M. Eryılmaz, H. Torul, U. Tamer, İ. H. Boyacı, Z. Ustundağ, *J. Colloid Interface Sci.*, 2013, **406**, 231-237.
- 46 B. Nikoobakht, M.A. El-Sayed, *Chem. Mater.*, 2003, **15**(10), 1957-1962.
- 110 47 M. Rycenga, J. M. McLellan, Y. Xia, *Chemical Physics Letters.*, 2009, **463**, 166-171.
- 48 N. Kanayama, H. Kitano, *Langmuir.*, 2000, **16**(2), 577-583.
- 115 49 Y. Erdoğdu, M.Tahir Güllüoğlu, M.Kurt, *J. Raman Spectrosc.*, 2000, **40**(11), 1615-1623.
- 50 M. Kurt, T.R. Sertbakan, M. Ozduran, M. Karabacak, *Journal of Molecular Structure.*, 2009, **921**, 178-187.
- 51 R. Ludwig, Y. Shiomi, S. Shinkai, *Langmuir.*, 1994, **10**(9), 3195-3200.
- 120 52 Ö. Torun, İ. Hakkı Boyacı, E. Temür, U. Tamer, *Biosensors and Bioelectronics.*, 2012, **37**(1), 53-60.
- 53 Y. Ling, N. Zhang, F. Qu, T. Wen, Z.F. Gao, N.B. Li, H.Q. Luo, *Spectrochimica Acta Part A: Molecular and Biomolecular Spectroscopy*, 2014, **118**(24), 315-320.
- 125 54 X. Wang, E. Liu, X. Zhang, *Electrochimica Acta*, 2014, **130**, 253-260.
- 55 R.K. Shervedani, A.H. Mehrjardi, N. Zamiri, *Bioelectrochemistry*, 2006, **69**, 201-208.
- 130 56 L. Jin, L. Shang, S. Guo, Y. Fang, D. Wen, L. Wang, J. Yin, S. Dong, *Biosensors and Bioelectronics*, 2011, **26**, 1965-1969.
- 57 P.N. Wahjudi, M.E. Patterson, S. Lim, J.K. Yee, C.S. Mao, W.N. P. Lee, *Clinical Biochemistry*, 2010, **43**(1-2), 198-207.
- 135 58 C. Ma, Z. Sun, C. Chen, L. Zhang, S. Zhu, *Food Chemistry*, 2014, **145**(15), 784-788.
- 59 K. V. Kong, Z. Lam, W. K. On Lau, W. K. Leong, M. Olivo, *J. Am. Chem. Soc.* 2013, **135**, 18028-18031.

- 1
2
3
4
5
6
7
8
9
10
11
12
13
14
15
16
17
18
19
20
21
22
23
24
25
26
27
28
29
30
31
32
33
34
35
36
37
38
39
40
41
42
43
44
45
46
47
48
49
50
51
52
53
54
55
56
57
58
59
60
- 60 Z. Alissa, W. Damon, L. Yichuan, W. Gongming, Y. Xuan, V. Boaz, S. Bakthan, G. Claire, L. Yat, *Science of Advanced Materials*, 2012, **4(10)**, 1047-1054(8).
- 61 I. Al-Ogaidi, H. Gou, A. K. A. Al-kazaz, Z. P. Aguilar, A. K. Melconian, P. Zheng, N. Wu, *Analytica. Chimica. Acta.*, 2014, **811**, 76– 80.
- 62 M. Rycenga, J. M. McLellan, Y. Xia, *Chemical Physics Letters*, 2008, **463**, 166–171.
- 63 Z. S. Wu, G. Z. Zhoua, J. H. Jiang, G. L. Shen, R. Q. Yu, *Talanta*, 2006, **70**, 533-539.

Figure Captions

Table 1. The comparison between the current systems in the literature and proposed SERS technique

Figure 1. The cyclic voltammograms of 100 mM ferrocyanide in water taken from the mixed monolayer of 3-MBA and 1-DT surface, scan rate: 100 mV/s. a) Bare gold electrode b) AuSAM–AuNPsSAM surfaces and c) AuSAM surface.

Figure 2. AFM images of a) Au surface, b) Au SAM and c) Au SAM–Au NPs SAM surfaces.

Figure 3. Raman spectrum of a) Au SAM–Au NPs SAM surface b) The decrease of the peak intensity at 1070 cm^{-1} when increasing glucose concentration was added to the Au SAM–Au NPs SAM surface.

Figure 4. SPR sensorgrams (gray lines) obtained for the binding of glucose in borate buffer at pH 9.0, to the a) Au SAMs and b) Au SAMs–Au NPs SAM, surface, which were fitted to the 1:1 Langmuir interaction model (black lines). All runs are overlaid for glucose concentrations at 2.8, 5.6, 11.1, and 22.2 μM .

Figure 5. Calibration curve obtained from change in the B–OH SERS signal at 1070 cm^{-1} , by varying the concentrations of glucose in buffer and blood reference material which were incubated on the surface.

Schemes

Scheme 1. Schematic illustration of the Au SAM–AuNPs SAM surface

Table1.

Applied techniques	LOD of glucose	The linear ranges for glucose
Fluorescence Spectroscopy ⁵³	8 μ M	0.01 mM to 0.1 mM
Non-Enzymatic Glucose Biosensor ⁵⁴	0.1 μ M	0.4 μ M to 12 mM
Electrochemical Impedance Spectroscopy ⁵⁵	0.016 mM	0 mM to 10 mM
Fluorescence Spectroscopy ⁵⁶	0.005 mM	0.01 mM to 0.5 mM
Gas Chromatography/Mass Spectroscopy ⁵⁷	0.3 μ M	0.05 mM to 1 mM
HPLC-ELSD ⁵⁸	0.4 μ M	1.1 mM to 11 mM
Triosmium carbonyl cluster-boronic acid - SERS ⁵⁹	0.1 mM	0.1 mM to 10 mM
Gold nanoparticle-coated zinc oxide nanowires - SERS ⁶⁰	0.25 mM	0.9 mM to 30 mM
Gold nanostar@SiO ₂ core-shell nanoparticles - SERS ⁶¹	16 μ M	25 μ M to 25 mM
1-dodecanethiol coated Ag nanocubes - SERS ⁶²	-	0 mM to 250 mM
Gold colloids modified by horseradish peroxidase and glucose oxidase - SERS ⁶³	0.46 mM	0.50 mM to 32 mM,
Developed SERS technique	0.5 mM	2 mM to 16 mM

5

10

15

20

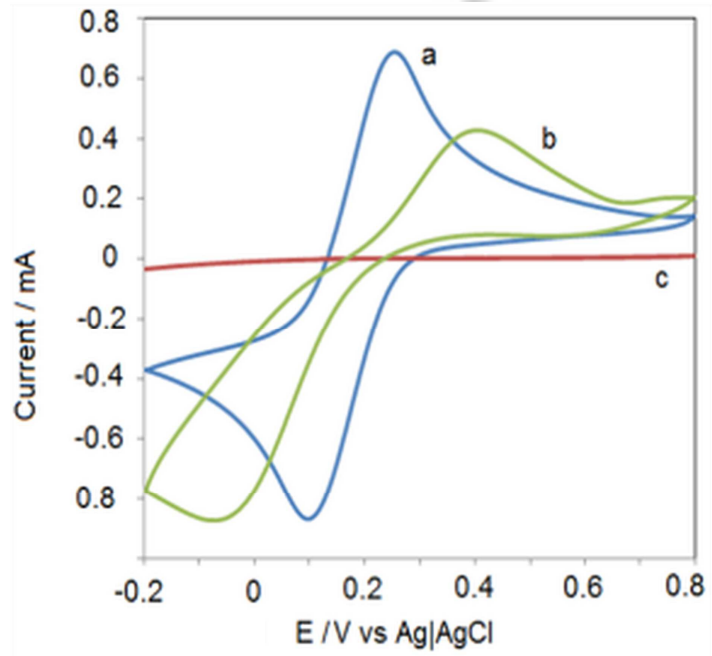
25

30

35

40

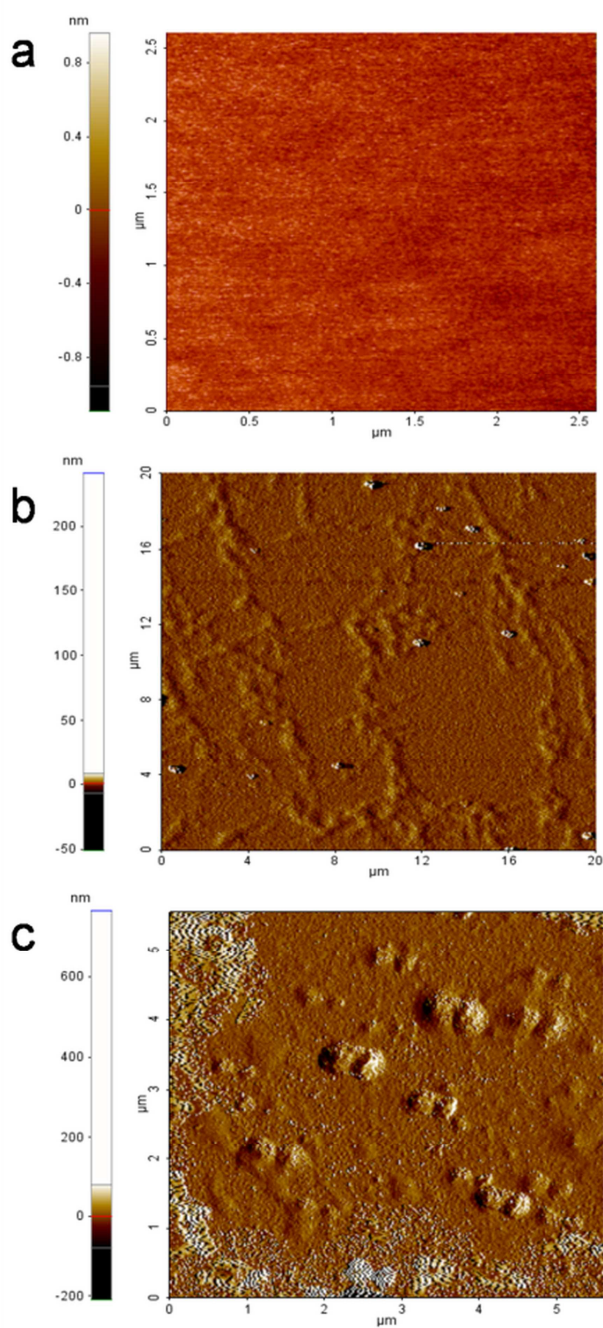
1
2
3
4
5
6
7
8
9
10
11
12
13
14
15
16
17
18
19
20
21
22
23
24
25
26
27
28
29
30
31
32
33
34
35
36
37
38
39
40
41
42
43
44
45
46
47
48
49
50
51
52
53
54
55
56
57
58
59
60



Analytical Methods Accepted Manuscript

Figure 2.

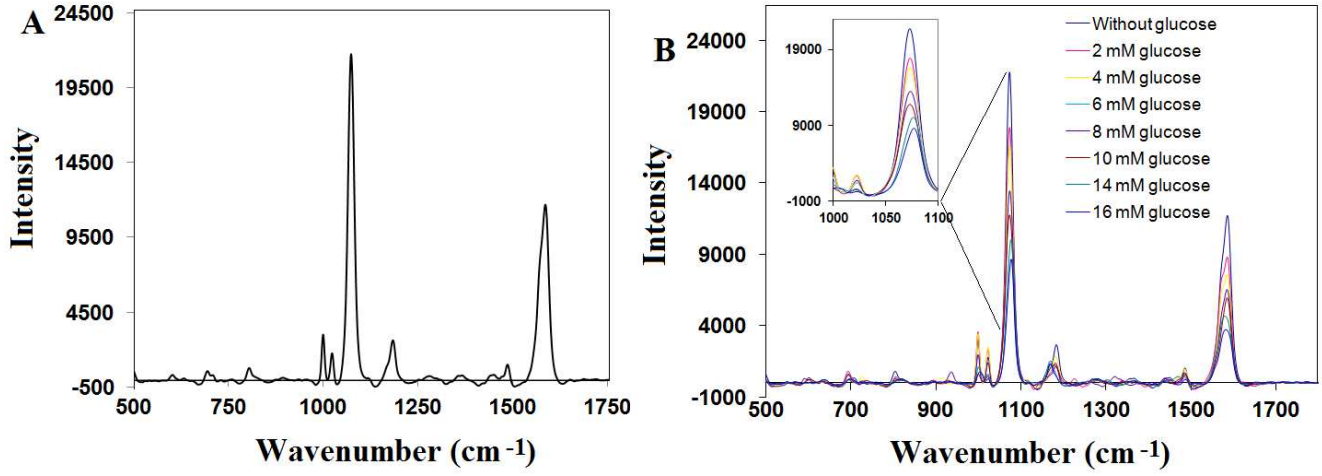
5



10

15

Figure 3.

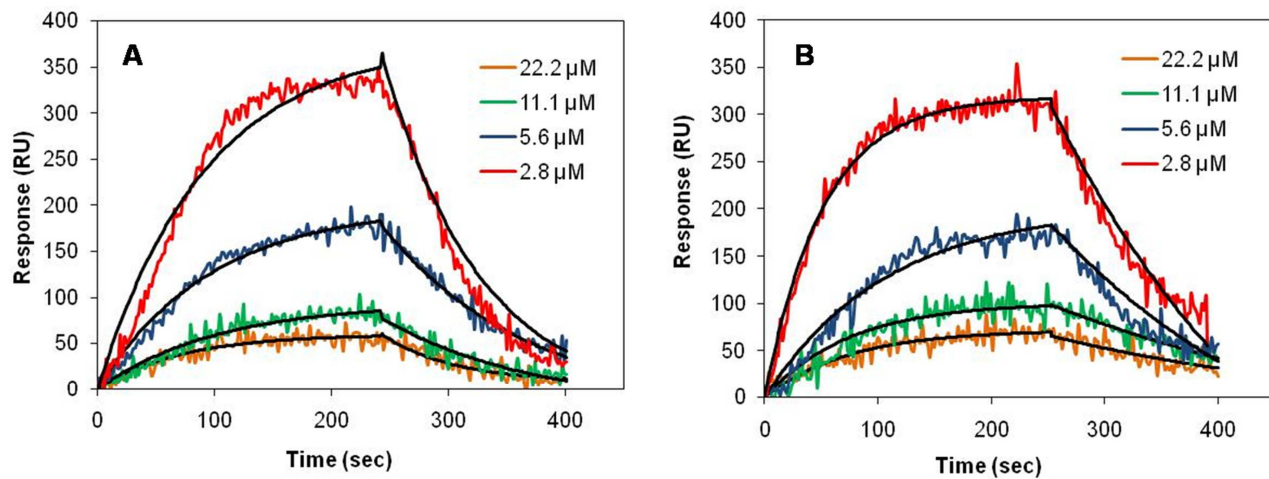


1
2
3
4
5
6
7
8
9
10
11
12
13
14
15
16
17
18
19
20
21
22
23
24
25
26
27
28
29
30
31
32
33
34
35
36
37
38
39
40
41
42
43
44
45
46
47
48
49
50
51
52
53
54
55
56
57
58
59
60

Analytical Methods Accepted Manuscript

Figure 4.

5



10

15

20

25

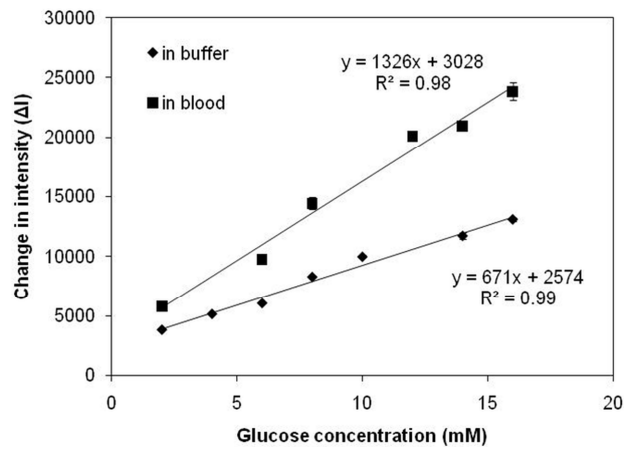
30

35

40

45

Figure 5.



1
2
3
4
5
6
7
8
9
10
11
12
13
14
15
16
17
18
19
20
21
22
23
24
25
26
27
28
29
30
31
32
33
34
35
36
37
38
39
40
41
42
43
44
45
46
47
48
49
50
51
52
53
54
55
56
57
58
59
60

5
10
15
20
25
30
35
40
45
50

Analytical Methods Accepted Manuscript

Scheme 1.

